

Characterization and quantification of Bcl-2 antisense G3139 and metabolites in plasma and urine by ion-pair reversed phase HPLC coupled with electrospray ion-trap mass spectrometry

Guowei Dai^{a,1}, Xiaohui Wei^a, Zhongfa Liu^a, Shujun Liu^b,
Guido Marcucci^{b,c}, Kenneth K. Chan^{a,c,*}

^a Division of Pharmaceutics, College of Pharmacy, Room no. 308, The Ohio State University, Comprehensive Cancer Center (OSU CCC), 410 W12th Ave., Columbus, OH 43210, USA

^b Division of Hematology–Oncology, College of Medicine and Public Health, The Ohio State University, Columbus, OH 43210, USA

^c Division of Human Cancer Genetics, College of Medicine and Public Health, The Ohio State University, Columbus, OH 43210, USA

Received 24 January 2005; accepted 24 May 2005

Available online 18 August 2005

Abstract

A novel ion-pair reversed phase electrospray ionization (IP-RP-ESI) liquid chromatography–mass spectrometry (LC–MS) method has been developed for identification and quantification of Bcl-2 antisense phosphorothioate oligonucleotides G3139 and metabolites in plasma. This method utilized solid phase extraction for desalting and matrix removal and detection by an ion trap mass spectrometer. Resolution was accomplished on a micro C18 column eluted with a mobile phase consisting of hexafluoro-2-propanol and triethylamine in methanol at 50 °C. Five G3139 metabolites were identified in plasma and urine from treated patients and rats. A cassette HPLC–MS/MS quantification method for G3139 and three metabolites was developed and validated with a limit of quantification (LOQ) of 17.6 nM in human and rat plasma with acceptable precision and accuracy. Plasma pharmacokinetics of G3139 and metabolites in these species were described.

© 2005 Elsevier B.V. All rights reserved.

Keywords: Pharmacokinetics; Tandem mass spectrometry; Metabolism; Bcl-2 antisense; N-in-one quantification

1. Introduction

With the advent of electrospray ionization (ESI) techniques, liquid chromatography–mass spectrometry (LC–MS)

has become a major qualitative and quantitative analytical tool for small organic molecules [1–3], peptides, and proteins [4–6]. For DNA, RNA, and oligonucleotides, this method has been less successful until relatively recently [7–9]. This is probably due to the lower sensitivity and several analytical problems associated with this type of molecules, such as: (1) inadequate chromatographic separation in either reversed phase or anion exchange chromatography, (2) lack of suitable ion-pairing reagents for both MS sensitivity and HPLC chromatography, and (3) extensive adduction with ubiquitous cations, such as sodium or potassium ions, in biological samples. While synthetic oligonucleotides have become increasingly important for diagnostic and therapeutic purposes, characterization of these compounds, monitoring of purity, and more importantly quantification of these compounds in biological matrices, and elucidation of metabolic products in preclinical and clinical evaluation are of paramount impor-

Abbreviations: HFIP, 1,1,1,3,3,3-hexafluoro-2-propanol; CVs, coefficients of variations; CID, collision induced dissociation; CIVI, continuous intravenous infusion; ESI, electrospray ionisation; ELISA, enzyme-linked immunosorbent assay; IP-RP-HPLC, ion-pair reversed phase HPLC chromatography; LOD, limit of detection; LOQ, limit of quantification; mRNA, messenger RNA; MRM, multiple reaction monitoring; ODNs, oligodeoxynucleotides; PK, pharmacokinetics; PS ODN, phosphorothioate oligonucleotide; SOS, Simple Oligonucleotide Sequencer; TEA, triethylamine; TEAA, triethylammonium acetate; TEAB, triethylammonium bicarbonate

* Corresponding author. Tel.: +1 614 292 8294; fax: +1 614 292 7766.

E-mail address: chan.56@osu.edu (K.K. Chan).

¹ Present address: Pharmaceutical Research Institute, Bristol-Myers Squibb Co., Princeton, NJ 08540, USA.

Table 1
Structures and molecular weight of G3139 and its metabolites identified in rat and human plasma

Identity	Proposed sequence (from 5' to 3')	Calculated M_w (Da)	Observed M_w (Da)			
			Human		Rat	
G3139	TCTCCAGCGTGCGCCAT	5684.9	+	5684.3	+	5684.0
M1 3' N-1	TCTCCAGCGTGCGCCA	5364.3	+	5364.0	+	5364.0
M2 3' N-2	TCTCCAGCGTGCGCC	5035.1	+	5034.0	+	5035.0
M3 3' N-3	TCTCCAGCGTGCGC	4729.8	+	4728.2	+	4730.0
M4 3' N-4	TCTCCAGCGTGCG	4424.6	+	4425.0	+	4424.7
M5 3' N-5	TCTCCAGCGTGC	4079.3	+	4078.6	+	4079.0
M6	Unknown peak ^a		+	Not oligonucleotide related	–	N/A
Internal standard	TCTCCAGCGTGCGCCAT CAGCATA	7944	N/A			

^a The peak was not detected in blank plasma but was detected as an ion at m/z 1911.

tance. In order to meet these demands, a number of strategies have now been developed with respect to solvent additives and modifiers [7,9,10], higher performance analytical sorbents and columns (particle size and new materials) [11,12], and improved instrumental parameters (flow rates and others) and manipulations (post column) [13–15] to improve resolution and sensitivity.

G3139 (Table 1), an 18-mer phosphorothioate oligonucleotide antisense designed to bind to the first six codons of the human Bcl-2 mRNA, is being investigated in multiple phases I–III clinical trials [16–19]. As high levels of the Bcl-2 were found associated with chemoresistance in malignant cells, the main hypothesis of these studies is that antisense down-regulation of its target would decrease the apoptosis threshold and induce chemotherapy sensitivity in otherwise chemoresistant disease. Preclinically, this compound has demonstrated a potent antisense activity in vitro and in vivo by downregulating Bcl-2 expression, resulting in increased tumor cell apoptosis, when administered alone or in combination with cytotoxic agents [20–22]. Chemosensitization effect of G3139 has been explored in patients with melanoma [23], hormone-refractory prostate cancer [19], chronic lymphocytic leukemia (CLL) [24], acute myeloid leukemia (AML) [18,25,26], and a variety of other tumors [16,27,28].

Although pharmacokinetics of G3139 has been reasonably well studied previously [18,29], and more recently by an ultra-sensitive non-LC–MS hybridization method [30,31], little is known about its metabolic fate, nor was there LC–MS quantitative method for G3139 and its metabolites. Previous published results regarding disposition of G3139 were based on radioactivity measurement, which did not readily separate parent drug from the metabolites, therefore generating little information concerning disposition of G3139 and its metabolites [32,33]. In fact, to date there were only two publications using LC–MS for quantification of antisense drugs in biological samples [34,35]. To overcome these problems, we first developed an ESI LC–MS method coupled to ion-pair reversed phase HPLC (IP-RP-HPLC) chromatography for separation and characterization of G3139 and three major metabolites. Further, we developed and validated a sensitive ESI LC–MS/MS N-in-one (cassette) quantification method

of G3139 and its metabolites in plasma, allowing characterization of G3139 and metabolite kinetics in human and in the rat.

2. Experimental

2.1. Materials and chemicals

G3139 was supplied by the National Cancer Institute (Bethesda, MD) and used without further purification. The internal standard (I.S.), a 25-mer phosphorothioate oligonucleotide, and other putative 3'-N-1, N-2, and N-3 of G3139 (here-to-fore G3139 is omitted) metabolites (Table 1) were obtained from Integrated DNA Technologies (Coralville, IA) and used without further purification. HPLC-grade methanol, triethylamine (TEA, 99.5%), triethylammonium bicarbonate (TEAB), and 1,1,1,3,3,3-hexafluoro-2-propanol (HFIP, 99.8%) were purchased from Aldrich (Milwaukee, WI, USA). A Milli-Q system (Millipore, Bedford, MA, USA) was used to prepare deionized water for HPLC analysis. The purity and identity of each ODN were verified by HPLC–UV–mass spectrometry (Finnigan LCQ, San Jose, CA). Blank human plasma was obtained from Red Cross (Columbus, OH). Drug-free rat plasma was purchased from Harlan Bio-products for Science Inc. (Indianapolis, IN, USA).

2.2. Instrumentation

The LC–MS system used consisted of a Finnigan (ThermoFinnigan, San Jose, CA) LCQ ion trap mass spectrometer coupled to a Shimadzu HPLC system (Shimadzu, Columbia, MD) and SPD-M10A PDA detector (Shimadzu, Columbia, MD). The HPLC system was equipped with two LC-10AD pumps, a SIL-10AD autoinjector (Shimadzu, Columbia, MD).

2.3. HPLC chromatographic and mass spectrometric conditions

An Xterra MS18 2.5- μ m (average pore diameter: 120 Å) 50 mm \times 2.1 mm stainless steel column (Waters Corp., Mil-

ford, MA) coupled to a MS C18 2.1 mm × 10 mm guard column (Waters Corp., Milford, MA) was used to separate G3139 and its metabolites. The HFIP-TEA buffer was prepared as a 200 mM stock solution as follows. To 10.5 mL of HFIP was added 485 mL water and 2 mL TEA with constant stirring for 1 h. The pH was then titrated to 8.35 with TEA and the final volume was adjusted to 500 mL. This stock solution was diluted to 100 mM with water and used as the A solvent (100 mM HFIP/8.6 mM TEA, pH 8.35) and with methanol and used as the mobile phase B (100 mM HFIP and 8.6 mM TEAB, pH 8.3). The column was kept at 50 °C in a column heater (Keystone, Woburn, MA) throughout the analysis. The components were eluted with a gradient mode at a flow rate of 0.20 mL/min. Gradient was initiated with 75% of solvent A, which was decreased to 50% in 30 min and returned to 25% B in 2 min. Prior to the next run, the column was equilibrated at 25% B for at least 8 min. The LC eluant was introduced into the electrospray ion source without splitting.

All experiments were carried out using the LCQ ion trap mass spectrometer with an ESI source operated in the negative ion mode. The electrospray high voltage was 2.0–2.2 kV. The temperature of the heated capillary was set at 210 °C. The mass spectrometer was operating with a background helium pressure of 1.75×10^{-3} Torr, a typical electrospray needle voltage of 4.5 kV, a sheath gas flow of 80 (arbitrary unit), and an auxiliary nitrogen gas flow of 30 (arbitrary unit). The mass spectrometer was tuned to its optimum sensitivity of charge states from $[M - 3H]^{3-}$ to $[M - 7H]^{7-}$ by infusion of either G3139 or 3' N-1 through N-3. All operations were controlled by Finnigan Xcalibur (Version 1.2) software in a Windows NT 4.0 system. The PDA was operated to give the spectra of 200–600 nm. All operations were controlled by EZstart 7.2 software in a Windows NT 4.0 system.

2.4. Sample preparation

Plasma samples were thawed and centrifuged at 1000 g for 5 min. Solid phase extraction (SPE) was used for isolation of G3139 and metabolites from plasma. Rat and human plasma samples spiked with appropriate amounts of pure compounds were used to construct calibration curves for G3139 and three major metabolites. Samples (0.2 mL) were then spiked with 20 µL of the I.S. at 400 µg/mL in water. Thereafter, the samples and standards were mixed with 0.8 mL of 0.1 M TEAB buffer and extracted on an Oasis HLB cartridge packed with 30 mg material (Waters, Corp., Milford, MA). The extraction tubes were conditioned first with 1 mL of acetonitrile followed by 1 mL of 0.1 M TEAB (pH 8.5). Then the samples mixed with 1 mL of 0.1 M TEAB were loaded onto each of the columns. The proteins and salts were removed by sequential washes with 2 mL of TEAB, 1 mL of 10% acetonitrile in 0.1 M TEAB and 1 mL of water by gravity flow. The breakthrough was examined by UV measurement and found to be negligible. Then the ODNs were eluted with 0.5 mL of 50% acetonitrile and the eluant was evaporated to dryness under a stream of nitrogen. The residue was reconstituted

with 100 µL of mobile phase A and 40 µL aliquot was analyzed by LC–MS.

2.5. Identification of major metabolites of G3139 in vivo

For HPLC analysis, the ion-pair elution described above was used with optimization for each run for maximum peak separation. Triple play mode (full scan, zoom scan, and MS/MS) [36,37] was chosen for identification of major metabolites of G3139 as follows: Full mass scan was in the range of 600–2000 Da, zoom scan was based on the most intense peak from the full scan mass spectrum, and data dependent tandem MS/MS was derived from the most intense peak. The MS/MS mass spectrum of metabolites of G3139 was acquired with 25–30% of the normalized collision energy with isolation width of 3.0 Da. Deconvolution was performed using Xcalibur BioMass to obtain the molecular mass information. Data of the MS/MS spectra of metabolites were exported from the Xcalibur Software (Finnigan, CA) and sequenced by an external computer program, Simple Oligonucleotide Sequencer (SOS) (Version 1.1) [38]. Comparison of the measured and predicted spectra was performed with the same program.

2.6. N-in-one quantification of G3139 and major metabolites in rat and human plasma

Multiple reaction monitoring (MRM) mode was employed for monitoring ion transitions for four analytes. ESI LC/mass spectra G3139 and three major metabolites were first obtained. The $[M - 3H]^{-3}$ ions of G3139 and three major metabolites were isolated and activated for 30 ms to produce daughter ions with optimized normalized collision energy of 15% for G3139 and three metabolites, 18% for internal standard. The ion transitions (SRM) monitored were m/z 1893.7³⁻ → 1842.8³⁻ for G3139, 1786.6³⁻ → 1736.3³⁻ for 3' N-1, 1676.7³⁻ → 1626.2³⁻ for 3' N-2, 1575.7³⁻ → 1524.6³⁻ for 3' N-3, and 1985.4⁴⁻ → 1947.5⁴⁻ for the I.S. An automatic gain control was set to ensure the high sensitivity, but avoiding the space charge effects. The mass spectrometer was tuned to its optimum sensitivity by flow infusion of G3139 at 20 µg/mL in 35% mobile phase B. All the operation was controlled by Finnigan Navigator 1.2 software on a Window NT 4.0 system.

2.7. Assay validation

Plasma samples for the standard curves were prepared by spiking 0.2 mL of rat and human plasma each with various amounts of G3139, three metabolites and a constant amount of the internal standard. The linearity was evaluated in the concentration range of 0.1–10 µg/mL. The within-day precision values were determined in five replicates at each concentration of 0.25, 1 and 5 µg/mL for each analyte. The between-day precision was determined across these three concentrations in five different days. The accuracy of the

assay was determined by comparing the nominal concentrations with the calculated values. The specificity of the assay was established by monitoring MRM for G3139 and each metabolite in blank plasma. The recovery of each analyte was estimated by comparing the peak area of the extract analyte to those of the unextracted at concentrations of 0.5 and 5 $\mu\text{g/mL}$.

2.8. Pharmacokinetic study of G3139 in Sprague–Dawley rats

Six Sprague–Dawley female rats weighing ~ 300 g (Harlan, Indianapolis, IN) were used in the pharmacokinetics studies. All animals were adapted to a 12-h light/dark cycle under controlled room temperature and humidity conditions. Food and water were given ad libitum. The animal facility is accredited by the American Association for Laboratory Animal Care. The study was performed with a protocol which adheres to the “Principles of Laboratory Animal Care” by NIH and approved by the Ohio State University Vivaria. The right jugular vein of each rat was cannulated under ketamine anesthesia (100 mg/kg), and the rat was allowed to recover for 12 h prior to drug administration. G3139 in sterile saline was given as an i.v. bolus dose at 20 mg/kg through the jugular vein cannula followed by flushing the cannula with 0.25 mL of normal saline. Approximately 0.2 mL each of heparinized blood was withdrawn according to a typical schedule of 0 (predose), 5, 10, 15, 30, 60, 120, 180, 240, 360, and 600 min after dosing, and the loss of fluid was replaced by flushing the cannula with an equal volume of normal saline. The blood samples were centrifuged at $10,000 \times g$ for 1 min and the supernatants of each were collected and kept frozen at -80°C until analysis. In a separate experiment, three rats were housed individually in metabolism cages that allowed for separate collection of urine and feces, and restricted to food only in the first 24 h after dosing. Urine samples were collected 24 h prior to dosing and at interval of 0–4, 4–8, 8–12, and 12–24 h after dosing. The total volume of urine was measured by weight difference and frozen at -80°C until analysis.

2.9. Data analysis

Plasma concentration–time data were analyzed by WinNonLin (Version 4.0, Pharsight Corporation, Mountain View, CA) via an appropriate pharmacokinetic model and relevant pharmacokinetic parameters of G3139 were obtained. For metabolites, noncompartmental analysis was used. Total body clearance, mean residence time (MRT), and steady-state volume of distribution (V_{ss}) were calculated as follows:

$$CL_T = \frac{\text{Dose}}{AUC_{0-\infty}} \quad (1)$$

$$MRT = \frac{AUMC}{AUC} \quad (2)$$

$$V_{\text{ss}} = MRT \times CL_T \quad (3)$$

where AUC and AUMC are the area under the concentration–time curve and area under the first moment curve.

3. Results

3.1. Identification of major metabolites of G3139 in vivo

The initial strategy involved characterization of the mass spectral fragmentation data of G3139. Fig. 1A shows the ESI LC/mass spectrum of G3139, which indicated a base $[M-3H]^{3-}$ at m/z 1893.7 and several ions at different charge states from -4 to -8 at lower intensities. Upon deconvolution, these multiple charged ions yielded the correct $[M-H]^-$ (m/z 5684.4) and associated isotope ions with $\pm 0.009\%$ mass accuracy, when compared to the calculated (m/z 5684.9) (Fig. 1B). Additionally, low level of sodium and potassium adduct ions were detected. Upon collision induced dissociation (CID) of $[M-3H]^{3-}$, the MS² spectrum gave fragment ions (Table 2), consistent with w and a-B series based on the literature information about the base sequence of oligonucleotides in ion trap mass spectrometry [39,40]. The oligonucleotide fragmentation nomenclature, as shown in Fig. 2, followed the widely accepted one proposed by McLuckey et al. [41]. The formation of the most abundant fragment ion at 1842.8 was readily accounted for by the loss

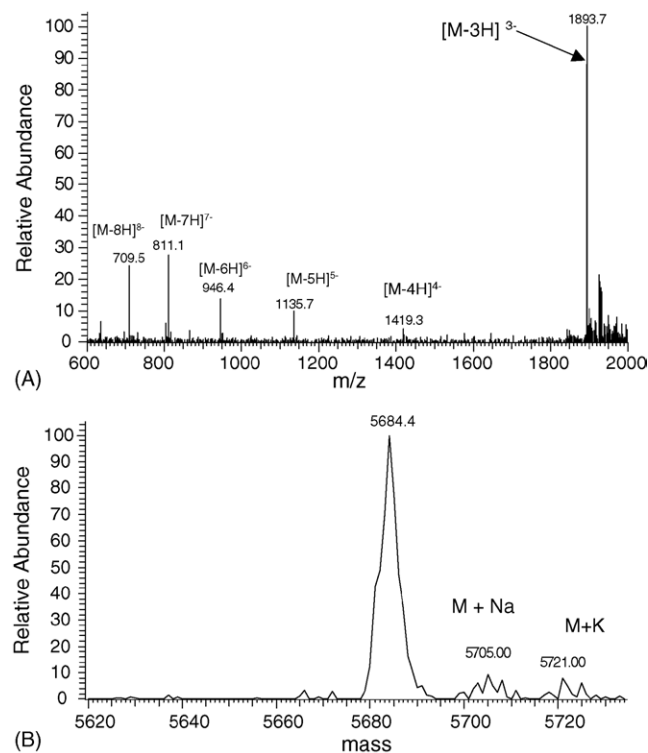


Fig. 1. ESI LC–MS mass spectrum (A) and the corresponding deconvoluted mass spectrum (B) of G3139. The charge states (-3 to -8) of the multiply charged ions are indicated above each ion in (A).

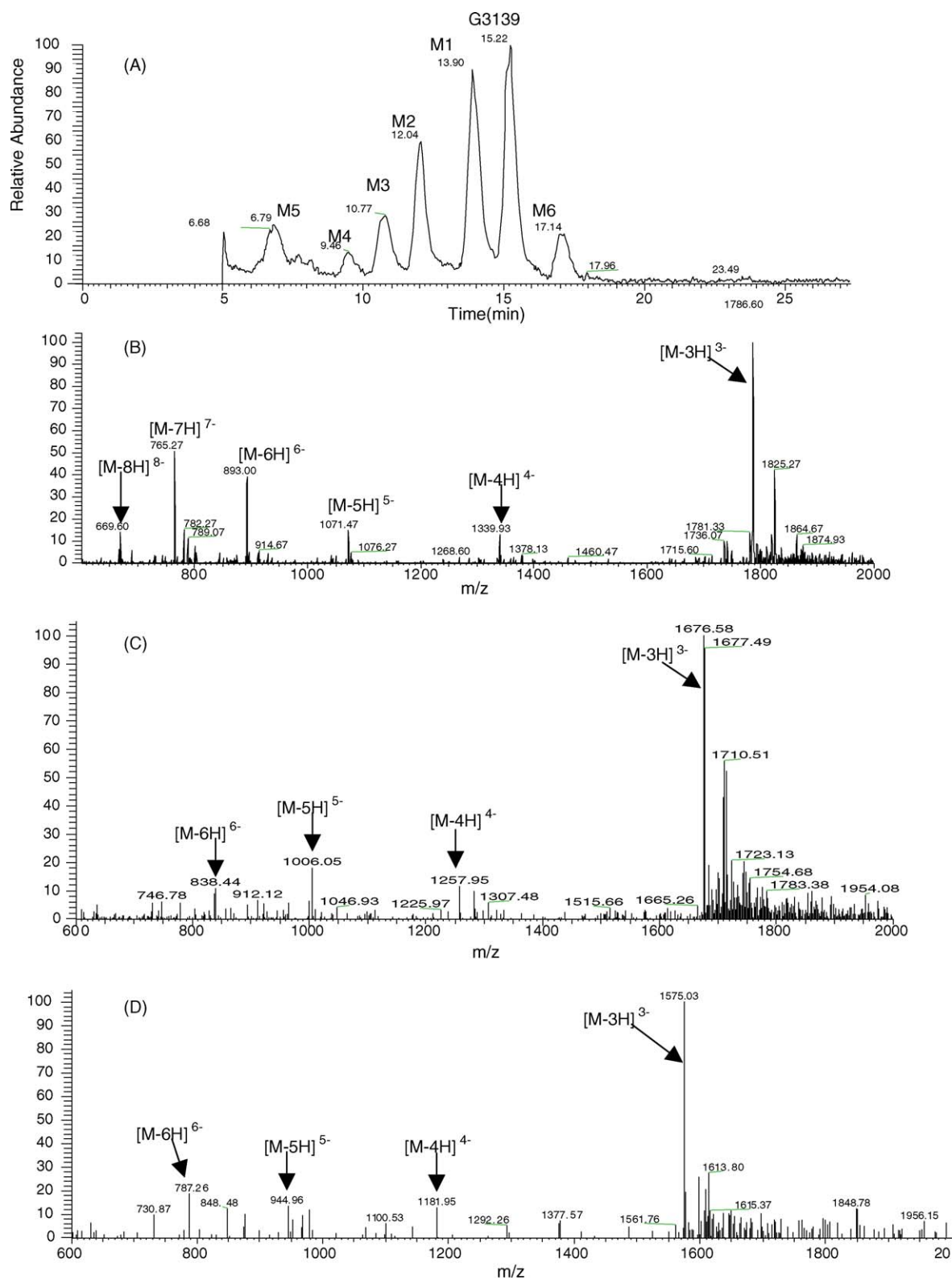
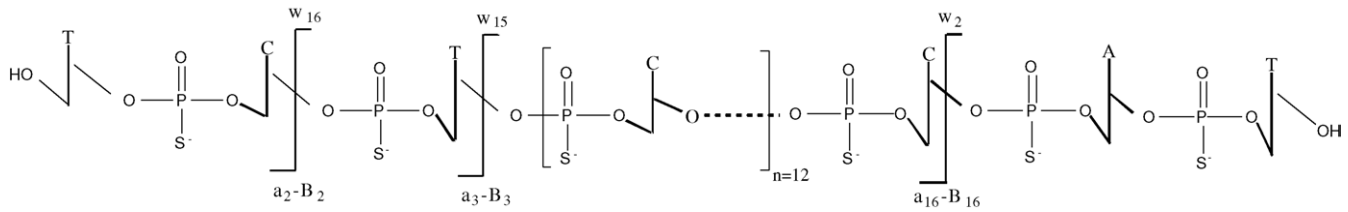


Fig. 2. A representative TIC of G3139 and major metabolites obtained from plasma extract of a patient treated with G3139 (A) and the mass spectra of 3' N-1 metabolite at retention time (RT) 13.90 min (B), of 3' N-2 metabolite at RT 12.04 min (C), of 3' N-3 metabolite at RT 10.7 min (D). Ions $[M - 3H]^{3-}$ to $[M - 8H]^{8-}$ were observed.

Table 2

Assignment of fragment ions obtained from collision-induced dissociation of $[M - 3H]^{3-}$ of G3139 at m/z 1893.7 in human plasma


m/z	Ion assignment	Sequence (from 5' to 3')	Relative intensity (%)
971	w_3^{-1}	CAT	24
1276	w_4^{-1}	CCAT	15
1621.1	w_5^{-1}	GCCAT	36
1926.2	w_6^{-1}	CGCCAT	9
1455.1	w_9^{-2}	GTGCGCCAT	8
1792.6	w_{11}^{-2}	GCGTGCGCCAT	4
1957	w_{12}^{-2}	AGCGTGCGCCAT	2
1615.5	w_{13}^{-3}	CCCAGCGTGCGCCAT	22
1717.7	w_{16}^{-3}	TCCCAGCGTGCGCCAT	10
1819	w_{17}^{-3}	CTCCCAGCGTGCGCCAT	8
1042.8	$a_4-B_4^{-1}$	TCTC	20
1347	$a_5-B_5^{-1}$	TCTCC	11
1652	$a_6-B_6^{-1}$	TCTCCC	5
1959	$a_7-B_7^{-1}$	TCTCCCA	3
1142	$a_8-B_8^{-2}$	TCTCCCAG	5
1092	$a_{11}-B_{11}^{-3}$	TCTCCCAGCGT	8
1800.9	$a_{12}-B_{12}^{-2}$	TCTCCCAGCGTG	5
1975	$a_{13}-B_{13}^{-2}$	TCTCCCAGCGTGC	37
1417.5	$a_{14}-B_{14}^{-3}$	TCTCCCAGCGTGCG	12
1634	$a_{16}-B_{16}^{-3}$	TCTCCCAGCGTGCGCC	10
1301.8	$a_{17}-B_{17}^{-4}$	TCTCCCAGCGTGCGCCA	20
1842.8	$(M - 3H-G)^{-3}$	TCTCCCAGCGTGCGCCAT	100

of neutral guanine base from the -3 charge state molecular ion (m/z 1893.7) (Table 2). The most diagnostic ions are w series that are used to determine the $3' \rightarrow 5'$ sequence and the a - B ions that are used to determine the $5' \rightarrow 3'$ sequence.

By comparing the plasma extract obtained from pretreatment (data not shown) with that obtained from the plasma sample in leukemia patient 120 h following i.v. infusion of G3139 at 7 mg/kg [25], six new peaks, denoted as M1, M2, M3, M4, M5, and M6 were found (Fig. 2A). The parent compound G3139 was eluted after its potential metabolites with a retention time of 15.2 min (Fig. 2A). The total ion current at the peak corresponding to M1 from 13.6 to 14.1 min was summed to generate the average mass spectrum (Fig. 2B), which shows several multiple charged ions. Following deconvolution, the molecular mass was found to be 5363.0 Da (Table 1). The most likely base composition for this mass was $d(C_8T_3A_2G_4)$, a loss of dT from G3139 $d(C_8T_4A_2G_4)$. Other possibilities of modified base or oxidative product were not supported by the mass computation. This component could be produced by either the $3'$ or $5'$ single nucleotide deletion from G3139. To distinguish these two possibilities, MS^2 spectra of $3'$ N-1 and $5'$ N-1 were obtained using the most abundant ion $[M - 3H]^{3-}$ at m/z 1786.7 and compared the same for M1 and the ions on the w series and the a - B ions. Eleven w ions and eight a - B ions generated from the MS^2 of

M1 were identified and assigned (Table 3). The MS^2 mass spectrum of M1 was essentially identical to that of $3'$ N-1 but not to $5'$ N-1, and these fragment ions are consistent with the fragmentation assignment of $3'$ N-1. Additionally, the MS^2 mass spectrum of $5'$ N-1 has distinct patterns of a - B ion and w ion series from that of $3'$ N-1. For example, the fragment ions as identified in MS^2 of $5'$ N-1 were w_2^{1-} (m/z 665.6), w_3^{1-} (m/z 970.9), and w_4^{1-} (m/z 1275.5), corresponding to sequences of $3'$ -AT, $3'$ -CAT, and $3'$ -CCAT, respectively, and were identified along with the a - B ions: $a_4-B_4^{-1}$ (m/z 1026.9), $a_6-B_6^{-1}$ (m/z 1661), and $a_{15}-B_{15}^{-3}$ (m/z 1628.9), corresponding to sequences of $5'$ -CTCC, $5'$ -CTCCCA, and $5'$ -CTCCCAGCGTGCGCC, respectively. This information further ruled out $5'$ N-1 as metabolite M1.

The second major peak (M2) in the plasma extract shows several multiple charged ions of different intensities (Fig. 2C), and upon deconvolution, gave a mass at m/z 5035.1 (Table 1). This mass shows a decrease of 649.3 Da from the parent compound, corresponding to a loss of two phosphorothioate nucleotides from the $3'$ end (-AT), but not from the $5'$ end (-TC). Indeed, the mass accuracy of M2 being 0.016% helps to exclude any other possible mass assignment. Thus, M2 was assigned as the metabolite derived from removal of two nucleotides from the $3'$ end or $3'$ N-2 of G3139 (Table 1). The sequence of M2 was further verified by the SOS program

Table 3

Assignment of fragment ions obtained from collision-induced dissociation of $[M - 3H]^{3-}$ of M1 at m/z 1786.8 in human plasma

m/z	Ion assignment	Sequence (from 5' to 3')	Relative intensity (%)
652.9	w_2^{-1}	CA	8
956.9	w_3^{-1}	CCA	14
803	w_4^{-2}	GCCA	2
956	w_5^{-2}	CGCCA	4
1150.1	w_7^{-2}	TGCGCCA	8
1461.2	w_9^{-2}	CGTGCGCCA	16
1634	w_{10}^{-2}	GCGTGCGCCA	18
1799.4	w_{11}^{-2}	AGCGTGCGCCA	15
1951	w_{12}^{-2}	CAGCGTGCGCCA	11
1610	w_{15}^{-3}	TCCCAGCGTGCGCCA	10
1711	w_{16}^{-3}	CTCCCAGCGTGCGCCA	22
723	$a_3-B_3^{-1}$	TCT	3
1042	$a_4-B_4^{-1}$	TCTC	15
1347.3	$a_5-B_5^{-1}$	TCTCC	25
1653	$a_6-B_6^{-1}$	TCTCCC	2
1959.6	$a_7-B_7^{-1}$	TCTCCCA	32
1640	$a_{11}-B_{11}^{-2}$	TCTCCCAGCGT	43
1531	$a_{15}-B_{15}^{-3}$	TCTCCCAGCGTGCGC	4
1635	$a_{16}-B_{16}^{-3}$	TCTCCCAGCGTGCGCC	31
1736.3	$(M - 3H-G)^{-3}$	TCTCCCAGCGTGCGCCA	100

(data not shown). MS² ions characteristic of M2 are of w ion series; for instance, w_2^{1-} (m/z 627), w_3^{1-} (m/z 917.9), w_5^{2-} (m/z 809.1), and w_7^{2-} (m/z 1143.0) corresponding to 3'-CC, 3'-GCC, 3'-GCGCC, and 3'-GTGCGCC, respectively. Fragment ions from the a-B ions were essentially the same as those from M1, suggesting M2 shares the same sequence with M1 from 5' terminal up to 15 nucleotides (data not shown).

Similarly, mass spectra of other major peaks are shown in Fig. 2. Ion envelopes were observed for all metabolites and in most cases $[M - 3H]^{3-}$ to $[M - 6]^{6-}$ were identifiable. Again, upon deconvolution molecular ions of these major components were obtained and M3, M4, and M5 were unambiguously assigned as 3' N-3, N-4, and N-5 with mass accuracy of 0.038, 0.023, and 0.017%, respectively (Table 1). One metabolite with the longest retention time (17.1 min) was not identified by ESI/MS/MS. This component did not seem to relate to an oligonucleotide based on the most abundant ion (m/z 1911.3), assuming that the ion was singly charged (data not shown).

Thus, based on this result, metabolism of G3139 probably involves mainly 3'-exonuclease cleavage consistent with metabolism of other antisense oligonucleotides [39,42,43].

Table 4

Urinary excretion of G3139 and its major metabolites in the rat following its i.v. bolus dose at 20 mg/kg

	G3139		3' N-1		3' N-2		3' N-3	
	0–4 h ^a	4–8 h ^a						
Amount excreted (μ g) (mean \pm S.D., $n = 3$)	161 \pm 13	4.87 \pm 1.76	58.7 \pm 4.87	2.88 \pm 0.8	84.5 \pm 31.3	2.05 \pm 1.05	46.6 \pm 6.0	2.67 \pm 2.0
Percentage of dose excreted in 24 h ^b ($n = 3$)	2.78		1.0		1.4		0.82	

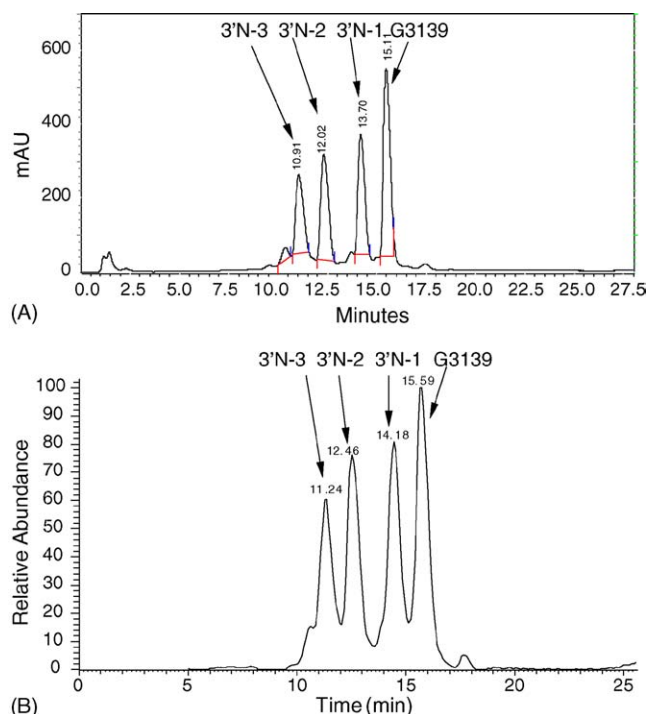
^a Collection period.^b Urine was collected to 24 h; however, no G3139 and metabolites were detected after 8 h.

Fig. 3. Representative IP-RP-HPLC-UV (A) and LC-MS total ion (TIC) chromatograms (B) of G3139, 3' N-1, 3' N-2, and 3' N-3 of G3139. UV was set at 260 nm.

Similarly, 3' N-1 to 3' N-5 were also identified in the 5 min plasma sample obtained from the rat given i.v. bolus of G3139 at 20 mg/kg and the results are summarized in Table 1. Similar pattern of metabolites was also observed in the 0–4 h urine extract taken from a rat given i.v. bolus of G3139 at 20 mg/kg (Table 4). 3 Selected ion monitoring (SIM) was performed and data for 3' N-1 up to 3' N-4 as well as G3139 were presented (data not shown).

3.2. N-in-one (cassette) quantification of G3139 and major metabolites in rat and human plasma

Using 100 mM HFIP combined with 8.6 mM TEA (pH 8.3) as the mobile phase with a gradient elution on a 2.5- μ m C18 reverse phase column (Xterra MS C18) at 50 °C, G3139, its 3' N-1, N-2, and N-3 were baseline resolved with UV detection (Fig. 3A), and with LC-MS they were nearly baseline separated (Fig. 4B). The slight change in resolution in MS was probably due to the peak broadening frequently encountered in the online serial connection. There was also a

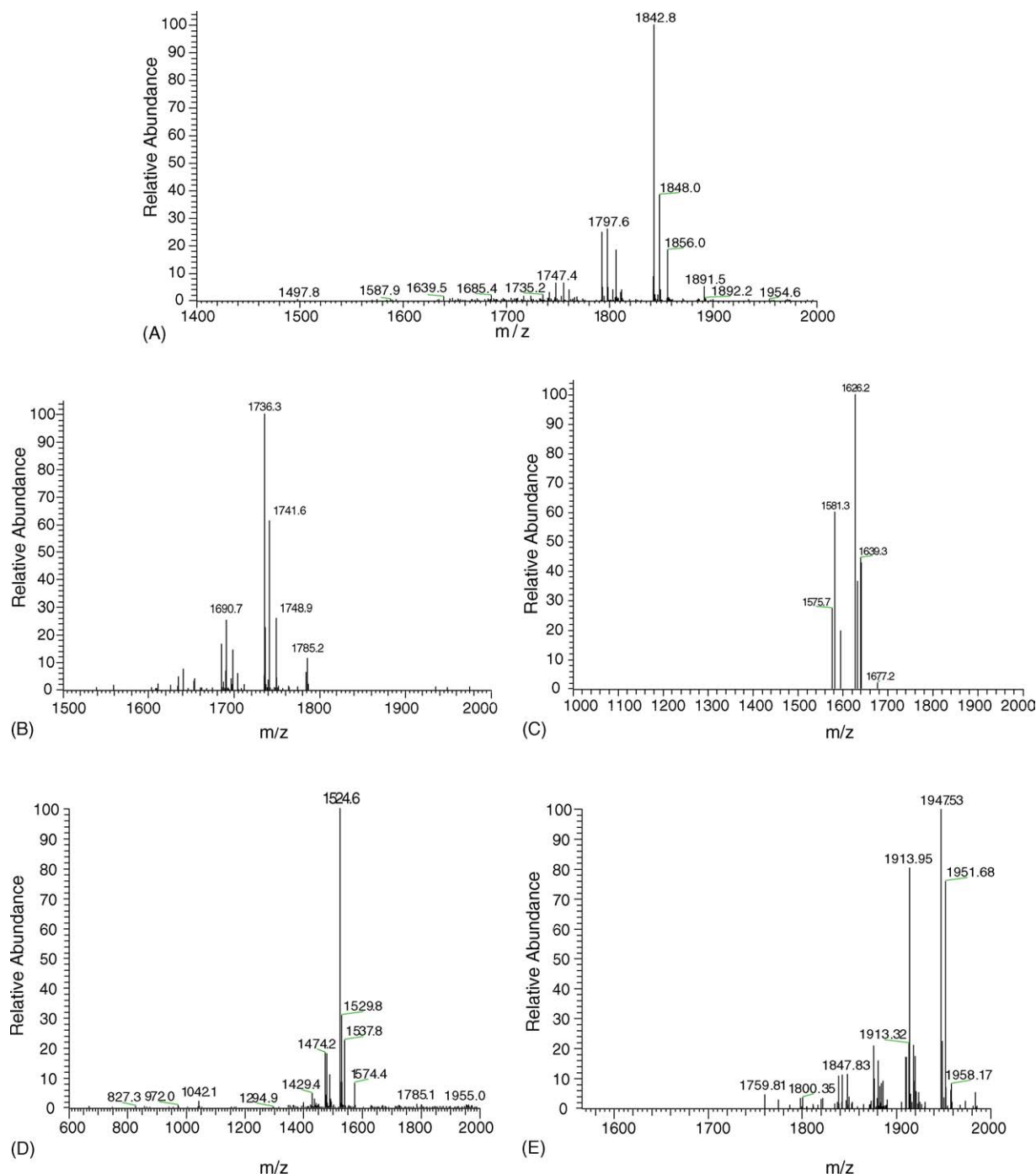


Fig. 4. CID spectra of the triply charged molecular ions of G3139 (A), of 3' N-1 (B), of 3' N-2 (C), of 3' N-3 (D), and of the internal standard (E). Ions at m/z 1842.8, m/z 1736.3, 1626.2, m/z 1524.6, and m/z 1947.5 represent the most abundant daughter ions from their parent $[M - 3H]^{-3}$ ions, respectively.

slight change in retention time due to matrix effect and slight change in flow rate.

As shown previously, under the HPLC–ESI/MS condition, G3139 gave a number of ions having different charge states, $[M - 8H]^{8-}$ (m/z 709.5), $[M - 7H]^{7-}$ (m/z 811.1), $[M - 6H]^{6-}$ (m/z 946.4), $[M - 5H]^{5-}$ (m/z 1135.7), $[M - 4H]^{4-}$ (m/z 1419.3), and $[M - 3H]^{3-}$ (m/z 1893.7, base ion) (Fig. 1A). The most intense triply charge state ion at m/z 1893.7 was selected for CID experiment which generated

four major daughter ions at m/z 1856, 1848, 1842.8, 1797.5, and 1747.4 (Fig. 4A). The parent/product ion pair at m/z 1893.7 and 1842.8 was chosen in the selected reaction monitoring (SRM) mode for quantification of G3139. Similarly, 3' N-1 generated the triply charged ion as the most abundant peak, $[M - 3H]^{3-}$ (m/z 1786.6) in the full scan mode and the major daughter ion under CID at m/z 1736.3 (Fig. 4B). The parent/product ion pair at m/z 1786.6 and 1736.3 was thus selected in the SRM mode for quantification of 3' N-

1. Similarly, ion pairs at m/z 1676.7/1626.2 (Fig. 4C) and at m/z 1575.6/1524.6 (Fig. 4D) were used in the SRM mode for quantification of 3' N-2 and 3' N-3, respectively. For the internal standard, the 25-mer ($M_w = 7945$) shows a parent/product ion pair at m/z 1985 and 1947.5 (Fig. 4E) and it was selected in the SRM mode for the internal standard measurement.

3.3. Assay validations

Having identified the G3139 metabolites and establishment for the conditions for the separation and monitoring of the parent compound and its metabolites and the internal standard, we then used this information for their quantification in human plasma and rat plasma. Representative MRM chromatograms of human plasma spiked with pure G3139, 3' N-1, N-2, N-3 each at concentration of 1 $\mu\text{g}/\text{mL}$ and I.S. of 20 $\mu\text{g}/\text{mL}$ are shown in Fig. 5. As shown, G3139, three major metabolites and the internal standard were baseline separated with no interference found from plasma at the same retention time under the SRM condition, thus further establishing the specificity of the assay.

The limit of quantification (LOQ) was set at 17.6 nM (100 ng/mL) in rat and human plasma, on the basis of a signal-to-noise level above 10:1. The recovery at 88 nM (0.5 $\mu\text{g}/\text{mL}$) ($n = 3$) was 34, 30, 32, and 54% for G3139, 3' N-1, 3' N-2, and 3' N-3, respectively. The recovery ($n = 3$) was 43, 58, 48, and 64% for G3139, 3' N-1, 3' N-2, and 3' N-3, respectively, at 880 nM (5 $\mu\text{g}/\text{mL}$). The assay was linear from 17.6 nM (100 ng/mL) to 1760 nM (10 $\mu\text{g}/\text{mL}$), using 0.2 mL rat plasma (figure not shown) and human plasma. The within-day precision, expressed as %CV is shown in Table 5A. As shown, the values ranged from 2.0 to 17.6 in rat plasma ($n = 5$) and 2.0 to 22% in human plasma with majority of the precision values fall below 15%. The accuracy values ranged

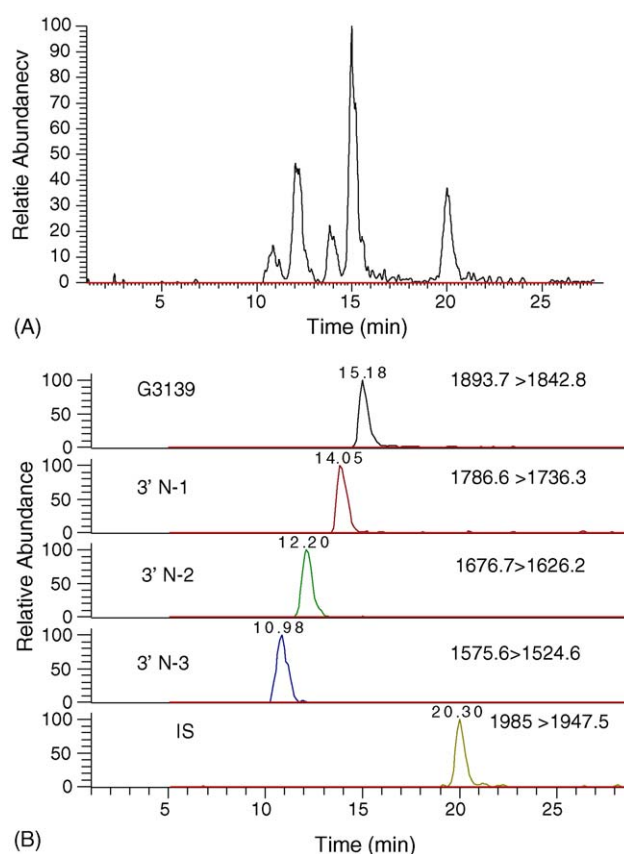


Fig. 5. A representative TIC in rat plasma spiked with 1 $\mu\text{g}/\text{mL}$ each of G3139 and three major metabolites and 20 $\mu\text{g}/\text{mL}$ internal standard (A), and its corresponding MRM chromatograms (B).

from 89 to 112%. The between-day CVs were 2–23% for 0.25, 1 and 5 $\mu\text{g}/\text{mL}$ with majority <15%. The accuracy values of the assay varied in the range from 82 to 126% with majority of the values between 89 and 115% (Table 5B).

Table 5A

Within-day assay validation characteristics of G3139 and three metabolites in rat and human plasma by IP-RP-HPLC coupled with ESI/MS

Concentrations in plasma, $\mu\text{g}/\text{mL}$ (nM) ^a ($n = 5$)		Rat plasma				Human plasma			
		G3139 ^b	N-1 ^b	N-2 ^b	N-3 ^b	G3139 ^b	N-1 ^b	N-2 ^b	N-3 ^b
0.25 (44)	Mean	0.24	0.24	0.25	0.27	0.24	0.26	0.23	0.26
	%CV	13.0	13.9	15.1	12.0	13.0	22.0	13.6	12.0
	Accuracy ^c	96	97	100	106	96	104	92	105
1 (176)	Mean	1.04	1.00	1.00	0.90	1.08	1.03	1.05	0.94
	%CV	12.2	17.6	4.0	11.8	5.5	12.0	4.7	3.5
	Accuracy ^c	104	100	100	90	108	103	105	94
5 (879)	Mean	4.84	4.72	4.71	4.98	4.53	4.47	4.71	4.98
	%CV	3.6	3.5	6.2	2.0	15.1	3.5	6.2	2.0
	Accuracy ^c	97	94	94	100	91	89	94	100
10 (1759)	Mean	9.84	11.0	10.6	11.2	NE	NE	NE	NE
	%CV	9.2	5.7	5.9	6.9	NE	NE	NE	NE
	Accuracy ^c	98	110	106	112	NE	NE	NE	NE

NE: not evaluated.

^a For G3139 only.

^b I.D.

^c Expressed as [(mean observed concentration/nominal concentration) \times 100].

Table 5B

Between-day assay validation characteristics of G3139 and three metabolites in rat and human plasma by IP-RP-HPLC coupled with ESI/MS

Concentrations in plasma, $\mu\text{g/mL}$ (nM) ^a ($n=5$)		Rat plasma				Human plasma			
		G3139 ^b	N-1 ^b	N-2 ^b	N-3 ^b	G3139 ^b	N-1 ^b	N-2 ^b	N-3 ^b
0.25 (44)	Mean	0.21	0.22	0.24	0.26	0.24	0.23	0.20	0.22
	%CV	23.0	17.0	21.3	20.9	7.1	18.8	9.0	17.0
	Accuracy	85	87	98	107	96	92	82	86
1 (176)	Mean	1.13	1.13	1.15	1.15	1.08	1.18	1.25	1.14
	%CV	13.3	9.2	9.3	9.1	10.5	8.0	5.9	14.0
	Accuracy	113	113	115	115	108	118	126	114
5 (879)	Mean	4.78	4.83	5.08	5.26	5.35	4.72	4.88	4.67
	%CV	4.6	6.5	9.4	6.3	6.3	10.7	2.0	6.3
	Accuracy	96	97	102	105	107	94	98	93

^a For G3139 only.^b I.D.

3.4. Pharmacokinetics of G3139 and three metabolites after i.v. bolus in SD rats

The method has been utilized for quantification of G3139 and three metabolites in the rat given a single bolus dose of G3139 at 20 mg/kg. All metabolites were detected as early as 5 min following dosing. Mean plasma concentration–time profiles of G3139 and metabolites in the rat are shown in Fig. 6A. As shown, plasma G3139 pharmacokinetics follows a bi-exponential decay. Plasma concentration–time data of G3139 were thus fitted to a two-compartment model with a first order elimination from the central compartment. A representative semi-logarithmic plot of the fitted curve is shown in Fig. 6B. The relevant pharmacokinetic parameters are thus computed and shown in Table 6. As shown, the mean total body clearance of G3139 was 3.74 ± 1.7 mL/min/kg (S.D., $n=5$). The harmonic means of half-lives were 8.6 (range 5–34) and 64.2 (range 49–101) min for α and β phases, respectively. The estimated V_{ss} was 217 mL/kg and V_1 was 103 mL/kg. The volume of central compartment (V_1)

Table 6

Relevant pharmacokinetic parameters of G3139 in the rat given as an i.v. bolus injection at 20 mg/kg (values are obtained from a two compartment i.v. bolus model, $n=5$)

Parameters (units)	Mean \pm S.D. (ranges) ($n=5$)
C_{max} ($\mu\text{g/mL}$)	200.7 ± 40.3
C_{5min} ($\mu\text{g/mL}$) ^a	145 ± 22.8
$AUC_{0-\infty}$ ($\mu\text{g min/mL}$)	6057 ± 2787
α (min^{-1})	0.081 ± 0.048
$t_{1/2\alpha}$ (min) ^b	8.6 (range: 5.2–34.7)
β (min^{-1})	0.0108 ± 0.003
$t_{1/2\beta}$ (min) ^b	64.2 (range: 49–101)
CL (mL/min/kg)	3.74 ± 1.7
V_1 (mL/kg)	103 ± 22
V_{ss} (mL/kg)	217 ± 37
MRT (min)	63 (35–109)
K10 (min^{-1})	0.042 ± 0.024
K12 (min^{-1})	0.030 ± 0.023
K21 (min^{-1})	0.021 ± 0.008

^a Observed plasma concentration of G3139 at 5 min.^b Harmonic mean.

is greater than the total blood volume of the rat but less than the total body water [44], suggesting G3139 distributed extensively in well-perfused organs such as liver and kidneys.

After 6 h post dose, plasma G3139 and metabolites levels fell below the LOQs of the assay. Levels of 3' N-1 reached a C_{max} of 28.9 ± 5.04 $\mu\text{g/mL}$, while the other two metabolites achieved their C_{max} of 13.76 and 12.0 $\mu\text{g/mL}$, respectively, all at about 11 min (Fig. 6 and Table 7). Following their peak

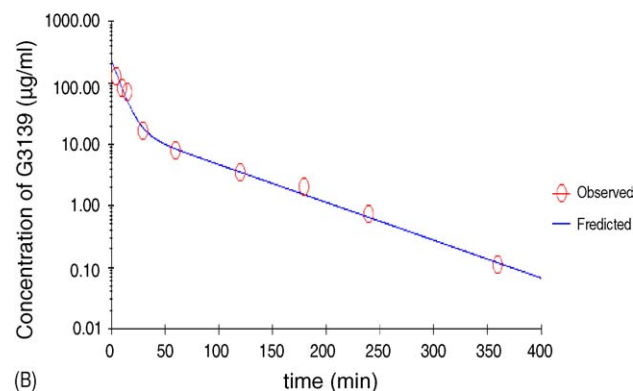
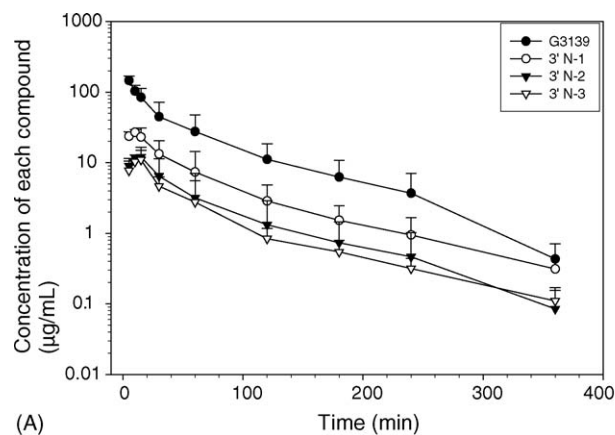


Fig. 6. (A) Plasma concentration–time profiles of G3139 and its major metabolites following i.v. bolus administration of 20 mg/kg G3139 in the rat. (B) A representative computer fitted plasma concentration–time profile of G3139 following i.v. bolus administration of 20 mg/kg G3139 in the rat.

Table 7

Relevant pharmacokinetic parameters of major metabolites of G3139 estimated by noncompartmental analysis in the rat ($n = 5$) given as an i.v. bolus injection of G3139 at 20 mg/kg

Metabolites	Parameters (units)	Estimates (mean \pm S.D.) ^a ($n = 5$)
3' N-1	AUC ($\mu\text{g min/mL}$)	1537 \pm 749
	%AUCm/AUCp ^b	25.0 \pm 7.0
	C_{max} ($\mu\text{g/mL}$)	28.94 \pm 5.04
	$t_{1/2,\lambda}$ (min)	63.6 (43.8–176)
	T_{max} (min)	11 \pm 2.2
	MRT (min)	82.8 \pm 49.5
3' N-2	AUC ($\mu\text{g min/mL}$)	707 \pm 524
	%AUCm/AUCp ^b	11.7 \pm 3.8
	C_{max} ($\mu\text{g/mL}$)	13.76 \pm 3.65
	$t_{1/2,\lambda}$ (min)	68.6 (42.7–139.7)
	T_{max} (min)	11.0 \pm 2.2
	MRT (min)	56.7 \pm 14.0
3' N-3	AUC ($\mu\text{g min/mL}$)	557 \pm 202
	%AUCm/AUCp ^b	9.88 \pm 3.60
	C_{max} ($\mu\text{g/mL}$)	12.07 \pm 3.32
	$t_{1/2,\lambda}$ (min)	69.8 (60–83)
	T_{max} (min)	11.1 \pm 2.3
	MRT (min)	60.5 \pm 10.3

^a From noncompartment analysis.

^b AUCm/AUCp: metabolite $\text{AUC}_{0-\infty}$ divided by parent drug $\text{AUC}_{0-\infty}$.

levels, plasma levels of the metabolites declined essentially in parallel to that of G3139. The relevant pharmacokinetic parameters of the metabolites were computed by noncompartmental analysis and are shown in Table 7. As shown, the harmonic means of the apparent terminal half-lives for 3' N-1, N-2 and N-3 G3139 were 63.6, 68.6 and 69.8 min, respectively, similar to that of the parent compound, suggesting formation-limited behaviors of the metabolites. The mean percentage AUCm/AUCp were 25, 11.7 and 9.9% for N-1, N-2, and N-3 G3139, respectively, indicating that the relative amounts of the metabolites, with the 3' N-1 being the major metabolite. Together, the metabolite levels represent nearly 50% of the total drug in circulation. It appears that urinary excretion of G3139 was only a minor pathway for elimination of plasma G3139 in the rat (Table 4). The parent drug was the most abundant species with 161 μg (S.D. = 13) excreted within the first 4 h and 4.87 μg excreted from 4 to 8 h after dosing with undetectable amounts thereafter. Small amounts of 3' N-1 (58.7 μg), 3' N-2 (84.5 μg), and 3' N-3 (46.6 μg) were detected in 4 h after dosing (Table 4) with undetectable amounts thereafter. The percent of administered dose recovered as oligonucleotides (G3139 + 3' N-1 + 3' N-2 + 3' N-3) in 24 h urine in the rat was only 6%.

4. Discussion

4.1. Sample preparation

In complex biological matrices, salts, small organic and inorganic molecules, and other protein and non-protein macromolecules further contribute to the difficulty in the

analysis of ODNs and PS ODNs because of matrix effects. Thus, sample preparation such as desalting and extraction of antisense molecules is still required for the success of their analysis. However, general precipitation method for ODNs with ammonium acetate or acetonitrile results in low recovery. Isolation of analytes by solid phase extraction with proper sorbent and eluants remains a useful and attractive approach. We have found that bulk interference matrices could be effectively removed by solid phase extraction with sequential elution with TEAB buffer, TEAB-acetonitrile, and water. The analytes were eluted with 50% acetonitrile with reasonable recovery.

4.2. Column selection

Oligonucleotides are usually separated by either anion-exchange or IP-RP-HPLC [45,46]. We and others have previously used HPLC–UV method with a strong anion exchange column with short length for the analysis of G3139 in plasma samples [17,18]. Although G3139 was separated from plasma matrix materials, resolution of G3139 from metabolites remained to be demonstrated. The use of a longer column will improve the resolution and would probably allow resolution with the metabolites. However, the high cost of the column makes the method unattractive and more importantly, the high salt content in the mobile phase renders the method impractical for the MS detection. On the other hand, the use of a reversed phase column in combination with mobile phase with ion-pairing property is an attractive alternative. After a number of attempts, we have chosen a C18 reversed phase column packed with a 2.5- μm fully porous C18 sorbent (Xterra MS C18). This column was specifically designed to tolerate high pH mobile phase so that the mobile phase at pH 8.3 did not seem to reduce the column lifetime. We also used an elevated temperature (50 $^{\circ}\text{C}$) to enhance the mass transfer and reduce the backpressure due to the fine particle of the column we used.

4.3. Mobile phase

Triethylammonium acetate buffer (TEAA) in acetonitrile is a commonly used buffer system for reversed phase ion pair separation of oligonucleotides. However, for MS analysis TEAA at concentrations at 50–100 mM has been shown to cause ion suppression due to its low volatility [9]. Apfel et al. suggested that HFIP/TEA could substitute TEAA in this buffer system and TEA could serve as an efficient ion pair reagent for the negatively charged phosphorothioate oligonucleotides. As the solvent is electrosprayed, HFIP, being a highly volatile weak acid (b.p. 57 $^{\circ}\text{C}$), separates from the surface of oligonucleotide-TEA (b.p. 89 $^{\circ}\text{C}$) complex in the source and the pH at the droplet surface rises toward 10 [9]. At this pH in gas phase, TEA dissociates from the oligonucleotide, which results in ionization of the ODNs. A buffer system with 16.3 mM TEA/400 mM HFIP (pH 7.0) in methanol was recommended for optimal LC–MS analy-

sis of oligonucleotides [9]. However, our results have shown that such combination of TEA/HFIP did not result in satisfactory performance on ESI/MS. Increasing pH of buffer by reducing concentration of HFIP to 100 mM (pH 8.3) reduced the charge state of G3139 and increased the abundance of $[M - 3H]^{3-}$ ions with other higher charge state ions <30% relative abundance of $[M - 3H]^{3-}$ ion. This result suggests that IP-RP-HPLC coupled with ESI is essential for characterization of metabolites of G3139 in complex biological samples since direct infusion into ESI/MS could not provide comparable sensitivity and mass accuracy due to cation adduct formation. The TEA serving as efficient ion pair reagent could displace cations adhered to the oligonucleotide phosphate backbone, thus resulting in superior deconvolution spectrum for G3139. It has been suggested that the TEA concentration rather than the concentration of HFIP plays a major role in the chromatography performance [47]. We found 100 mM HFIP combined with 8.6 mM TEA (pH 8.3) appears to offer the best ion pair efficiency and MS performance. Similar finding was also reported by Gilar and coworkers [47]. Additionally, the current TEA/HFIP solvent system appears to reduce the cation adductions, as only low sodium and potassium adduct ions were detected.

4.4. Mass spectrometry

Characterization of molecular composition of metabolites relies on high accuracy in molecular mass measurements. It has been reported previously that ESI ion trap mass spectrometry provided mass accuracy ranging from 0.2 to 1.2 Da for small oligonucleotides and ranging from 0.1 to 6.4 Da for PCR products (20000–26000 Da) [48,49]. Using a LCQ ion trap instrument, we have found that the mass accuracy was $\pm 0.009\%$. Deconvolution readily yielded the unambiguous structural verification. Using this instrument, we were able to identify most metabolites of G3139 in biological samples following a single injection, with better than 300 ppm mass accuracy. Identification of majority of metabolites was straightforward by comparing ion envelope generated with theoretical one and deconvolution calculation. However, since both 3' and 5'-terminals of G3139 are deoxyribo-thymine (dT), 3' N-1 and 5' N-1 from M1 have exactly the same ion envelope and molecular mass upon deconvolution measurement and both cannot be readily differentiated. Fortunately, algorithm for interpretation of CID mass spectra of oligonucleotides based on mass spectral fragmentation data has been developed for unknown nucleotides [38,41,50]. This strategy was initially developed by McLuckey and co-workers [41] and the software was recently reported by McClosky based on fragmentation chemistry of oligonucleotides under ESI/MS/MS [38]. We have used this interactive Simple Oligonucleotide Sequencer (SOS) [38] to successfully elucidate and confirm the sequencing of M1 from MS/MS spectra. The extensive information obtained by data dependent scan provided a new strategy for characterization of metabolites of G3139. Our results indicate that the major metabolic pathway for G3139

is hydrolysis of the parent drug probably by 3' exonuclease existing in various tissues including plasma. Further, mouse, rat and human exhibited very similar plasma metabolism (data not shown for the mouse). Using the similar approach, we have also detected these three metabolites in rat urine, but the levels were only measurable for 8 h.

Using this optimized HPLC–MS condition, a novel quantification method was developed to simultaneously quantify parent drug as well as major metabolites as “N in one” or in a cassette fashion. Synthetic G3139 and three major metabolites were used to construct calibration curves and the assay was found to be linear over the range of 17.6 nM (100 ng/mL)–1760 nM (10 μ g/mL). In comparison to LC–UV, LC–MS method clearly is more sensitive and specific. Although the novel hybridization ELISA assay previously developed in our laboratory provided higher sensitivity, allowing measurement of intracellular drug levels [30,31,51], it was not capable of determining various metabolites levels in biological fluids. Other previous pharmacokinetics and metabolism studies of oligonucleotides based primarily on radiolabel method were also incapable of differentiating parent drug from metabolites. We have developed and validated a novel HPLC–MS/MS method to simultaneously quantify parent drug and metabolites in plasma. The between-run and within-run precision and accuracy of this ESI HPLC–MS/MS method in rat and human plasma are acceptable with LOQ of 17.6, 18.6, 20, and 21 nM (0.1 μ g/mL) for G3139, 3' N-1, 3' N-2, and 3' N-3, respectively, in rat or human plasma. Using this novel and validated method, we found that G3139 was rapidly metabolized to 3' N-1 by 3' probably by exonucleases in rat and human. The rapid appearance of peak levels, the essentially parallel plasma concentration time profiles, and similar terminal half-lives relative to G3139 of the metabolites indicate either that metabolite kinetics is formation-limited or that the metabolites may have similar elimination characteristics to G3139, a possible existence of flip-flop kinetics [52].

5. Conclusion

In conclusion, a novel ion-pair reverse-phase ESI HPLC–MS method has been developed for identification and quantification of major metabolites of G3139 in vivo. TEA/HFIP is a useful additive in the method for the analysis of PS ODNs. Metabolism of G3139 in vivo is probably primarily mediated by 3' exonuclease in the rat and human. Using this validated method, the disposition of G3139 in rat was found to be best fit with a two-compartment model and metabolites disposition may follow formation-limited or flip-flop kinetics.

Acknowledgements

We thank Drs. Jef Rozenski (Katholieke Universiteit Leuven, Belgium) and James A. McCloskey (University of Utah)

for providing the SOS program used in this work. This research was supported in part by grants R21 CA94552 from the National Cancer Institute, the National Institute of Health and by BioMedical Mass Spectrometry Laboratory of College of Pharmacy.

References

- [1] Z. Li, K.K. Chan, *J. Pharm. Biomed. Anal.* 22 (2000) 33.
- [2] Z. Liu, H.G. Floss, J.M. Cassady, J. Xiao, K.K. Chan, *J. Pharm. Biomed. Anal.* 36 (2004) 815.
- [3] C.M. Chavez-Eng, M.L. Constanzer, B.K. Matuszewski, *J. Chromatogr. B Biomed. Sci. Appl.* 748 (2000) 31.
- [4] W.Y. Feng, K.K. Chan, J.M. Covey, *J. Pharm. Biomed. Anal.* 28 (2002) 601.
- [5] J.C. Le Blanc, J.W. Hager, A.M. Ilisiu, C. Hunter, F. Zhong, I. Chu, *Proteomics* 3 (2003) 859.
- [6] D.C. Delinsky, K.T. Hill, C.A. White, M.G. Bartlett, *Rapid Commun. Mass Spectrom.* 18 (2004) 293.
- [7] N. Potier, A. Van Dorsselaer, Y. Cordier, O. Roch, R. Bischoff, *Nucleic Acids Res.* 22 (1994) 3895.
- [8] M. Greig, R.H. Griffey, *Rapid Commun. Mass Spectrom.* 9 (1995) 97.
- [9] A. Apffel, J.A. Chakel, S. Fischer, K. Lichtenwalter, W.S. Hancock, *Anal. Chem.* 69 (1997) 1320.
- [10] D.C. Muddiman, *J. Am. Soc. Mass Spectrom.* 7 (1996) 697.
- [11] C.G. Huber, M.R. Buchmeiser, *Anal. Chem.* 70 (1998) 5288.
- [12] W. Walcher, H. Oberacher, S. Troiani, G. Holzl, P. Oefner, L. Zolla, C.G. Huber, *J. Chromatogr. B Anal. Technol. Biomed. Life Sci.* 782 (2002) 111.
- [13] C.G. Huber, A. Krajete, *J. Chromatogr. A* 870 (2000) 413.
- [14] K. Deguchi, M. Ishikawa, T. Yokokura, I. Ogata, S. Ito, T. Mimura, C. Ostrander, *Rapid Commun. Mass Spectrom.* 16 (2002) 2133.
- [15] A.V. Willems, D.L. Deforce, W.E. Lambert, C.H. Van Peteghem, J.F. Van Bocxlaer, *J. Chromatogr. A* 1052 (2004) 93.
- [16] K.N. Chi, M.E. Gleave, R. Klasa, N. Murray, C. Bryce, D.E. Lopes de Menezes, S. D'Aloisio, A.W. Tolcher, *Clin. Cancer Res.* 7 (2001) 3920.
- [17] M.J. Morris, W.P. Tong, C. Cordon-Cardo, M. Drobnjak, W.K. Kelly, S.F. Slovin, K.L. Terry, K. Siedlecki, P. Swanson, M. Rafi, R.S. DiPaola, N. Rosen, H.I. Scher, *Clin. Cancer Res.* 8 (2002) 679.
- [18] G. Marcucci, J.C. Byrd, G. Dai, M.I. Klisovic, P.J. Kourlas, D.C. Young, S.R. Cataland, D.B. Fisher, D. Lucas, K.K. Chan, P. Porcu, Z.P. Lin, S.F. Farag, S.R. Frankel, J.A. Zwiebel, E.H. Kraut, S.P. Balcerzak, C.D. Bloomfield, M.R. Grever, M.A. Caligiuri, *Blood* 101 (2003) 425.
- [19] A.W. Tolcher, J. Kuhn, G. Schwartz, A. Patnaik, L.A. Hammond, I. Thompson, H. Fingert, D. Bushnell, S. Malik, J. Kreisberg, E. Izbicka, L. Smetzer, E.K. Rowinsky, *Clin. Cancer Res.* 10 (2004) 5048.
- [20] F.E. Cotter, P. Johnson, P. Hall, C. Pocock, N. al Mahdi, J.K. Cowell, G. Morgan, *Oncogene* 9 (1994) 3049.
- [21] M. Konopleva, A.M. Tari, Z. Estrov, D. Harris, Z. Xie, S. Zhao, G. Lopez-Berestein, M. Andreeff, *Blood* 95 (2000) 3929.
- [22] B. Jansen, H. Schlagbauer-Wadl, B.D. Brown, R.N. Bryan, A. van Elsas, M. Muller, K. Wolff, H.G. Eichler, H. Pehamberger, *Nat. Med.* 4 (1998) 232.
- [23] B. Jansen, V. Wacheck, E. Heere-Ress, H. Schlagbauer-Wadl, C. Hoeller, T. Lucas, M. Hoermann, U. Hollenstein, K. Wolff, H. Pehamberger, *Lancet* 356 (2000) 1728.
- [24] K.R. Rai, J.O. Moore, T.E. Boyd, L.M. Larratt, A.K. Golenkov, B. Koziner, R.G. Bociek, L.M. Itri, *Blood* 104 (2004) 338.
- [25] G. Marcucci, G. Dai, M.I. Klisovic, T.S. Shen, S. Liu, D.A. Sher, D. Lucas, S.P. Whitman, J.A. Zwiebel, S.R. Frankel, M.R. Grever, W.Y. Stock, K.K. Chan, J.C. Byrd, *Blood* 102 (2003) 874a.
- [26] G. Marcucci, W. Stock, G. Dai, M.I. Klisovic, K. Maharry, T. Shen, S. Liu, D.A. Sher, D. Lucas, A. Zwiebel, R.A. Larson, M.A. Caligiuri, C.D. Bloomfield, K.K. Chan, M.R. Grever, J.C. Byrd, *Ann. Hematol.* 83 (Suppl. 1) (2004) S93.
- [27] C.M. Rudin, M. Kozloff, P.C. Hoffman, M.J. Edelman, R. Karnauskas, R. Tomek, L. Szeto, E.E. Vokes, *J. Clin. Oncol.* 22 (2004) 1110.
- [28] J. Marshall, H. Chen, D. Yang, M. Figueira, K.B. Bouker, Y. Ling, M. Lippman, S.R. Frankel, D.F. Hayes, *Ann. Oncol.* 15 (2004) 1274.
- [29] F.I. Raynaud, R.M. Orr, P.M. Goddard, H.A. Lacey, H. Lancashire, I.R. Judson, T. Beck, B. Bryan, F.E. Cotter, *J. Pharmacol. Exp. Ther.* 281 (1997) 420.
- [30] G. Dai, K.K. Chan, D. Hoyt, T. Shen, M. Grever, M. Caligiuri, J. Byrd, G. Marcucci, *Proc. Am. Assoc. Cancer Res.* 44 (2003) 1299 (abstract 6500).
- [31] G. Dai, K.K. Chan, S. Liu, D. Hoyt, S. Whitman, M. Klisovic, T. Shen, M.A. Caligiuri, J.C. Byrd, M. Grever, G. Marcucci, *Clin. Cancer Res.* 11 (2005) 2998.
- [32] F.I. Raynaud, R.M. Orr, P.M. Goddard, H.A. Lacey, H. Lancashire, I.R. Judson, T. Beck, B. Bryan, F.E. Cotter, *J. Pharmacol. Exp. Ther.* 281 (1997) 420.
- [33] D.E. Lopes de Menezes, N. Hudon, N. McIntosh, L.D. Mayer, *Clin. Cancer Res.* 6 (2000) 2891.
- [34] A. Ahmad, S. Khan, I. Ahmad, *Methods Enzymol.* 387 (2004) 230.
- [35] J.L. Johnson, W. Guo, J. Zang, S. Khan, S.A. Bardin, A. Ahmad, J.X. Duggan, I. Ahmad, *Biomed. Chromatogr.* 19 (2005) 272.
- [36] Z. Liu, P.E. Minkler, D. Lin, L.M. Sayre, *Rapid Commun. Mass Spectrom.* 18 (2004) 1059.
- [37] Z. Liu, H.G. Floss, J.M. Cassady, K.K. Chan, *J. Mass Spectrom.* 40 (2005) 389.
- [38] J. Rozenski, J.A. McCloskey, *J. Am. Soc. Mass Spectrom.* 13 (2002) 200.
- [39] R.H. Griffey, M.J. Greig, H.J. Gaus, K. Liu, D. Monteith, M. Winniman, L.L. Cummins, *J. Mass Spectrom.* 32 (1997) 305.
- [40] S.A. McLuckey, D.E. Goeringer, G.L. Glish, *Anal. Chem.* 64 (1992) 1455.
- [41] S.A. McLuckey, G.L. Glish, G.J. Van Berkel, *Anal. Chem.* 63 (1991) 1971.
- [42] J. Temsamani, J.Y. Tang, S. Agrawal, *Ann. N. Y. Acad. Sci.* 660 (1992) 318.
- [43] A.S. Cohen, A.J. Bourque, B.H. Wang, D.L. Smisek, A. Belenky, *Antisense Nucleic Acid Drug Dev.* 7 (1997) 13.
- [44] B. Davies, T. Morris, *Pharm. Res.* 10 (1993) 1093.
- [45] A. Apffel, J.A. Chakel, S. Fischer, K. Lichtenwalter, W.S. Hancock, *J. Chromatogr. A* 777 (1997) 3.
- [46] V. Metelev, S. Agrawal, *Anal. Biochem.* 200 (1992) 342.
- [47] M. Gilar, *Anal. Biochem.* 298 (2001) 196.
- [48] A. Premstaller, H. Oberacher, C.G. Huber, *Anal. Chem.* 72 (2000) 4386.
- [49] H. Oberacher, W. Parson, R. Muhlmann, C.G. Huber, *Anal. Chem.* 73 (2001) 5109.
- [50] J. Ni, C. Pomerantz, J. Rozenski, Y. Zhang, J.A. McCloskey, *Anal. Chem.* 68 (1996) 1989.
- [51] G. Marcucci, W. Stock, G. Dai, S. Liu, M.I. Klisovic, W. Blum, C. Kefauver, D.A. Sher, M. Green, M. Moran, C.D. Bloomfield, J.A. Zwiebel, R.A. Larson, M.R. Grever, K.K. Chan, J.C. Byrd, *J. Clin. Oncol.* 23 (2005) 3404.
- [52] K.K. Chan, *Drug Metab. Dispos.* 10 (1982) 474.